EXPERIMENTAL INVESTIGATION ON FREE VIBRATIONAL DAMPING AND DRILLING BEHAVIOR OF FLAX REINFORCED EPOXY COMPOSITES USING ADAPTIVE NEURO FUZZY INFERENCE SYSTEM

SHETTAHALLI MANTAIAH VINU KUMAR,[*] RENGARAJ JEYAKUMAR,[**] NALLASIVAM MANIKANDAPRABU[***] and CHANDRASEKARAN SASIKUMAR[****]

[*]*Department of Mechanical Engineering, Sri Krishna College of Technology-Kovaipudur, Coimbatore-42, India*
[**]*Department of Mechanical Engineering, Sri Krishna College of Engineering and Technology-Kuniyamuthur, Coimbatore-08, India*
[***]*Department of Electronics and Communication Engineering, Sri Krishna College of Technology-Kovaipudur, Coimbatore-42, India*
[****]*Department of Mechanical Engineering, Bannari Amman Institute of Technology, Sathyamangalam, Tamil Nadu, India*
✉ *Corresponding author: S. M. Vinu Kumar, vinukmr1988@gmail.com*

Received April 8, 2024

Flax reinforced epoxy (F-Ep) composites were prepared by the compression moulding technique, varying the fiber content (0, 25, 35 and 45 wt%). The free vibration test was performed on the neat epoxy and F-Ep composites to understand their dynamic characteristics, and results showed that natural frequency and damping factor of the F-Ep composites increased with an increase in the fiber content. The F-Ep composite (45F-Ep) that exhibited better damping was selected for performing the drilling operation. Factors such as spindle speed (rpm), feed rate (mm/min) and drill point angle (degree) were chosen as input parameters and the tabulated set of experiments were in accordance with Taguchi's design of experiment. The response measured was thrust force and the obtained values were found in the range of 19.66 to 50.75 N. The minimum value of thrust force was achieved when the F-Ep composite was drilled at high spindle speed (3000 rpm), with a feed rate of 75 mm/min using the drill point angle of 118°. ANOVA analysis showed that the developed regression model was significant and thrust force was mainly influenced by the spindle speed. Mathematical models were developed for drilling F-Ep composite using response surface methodology (RSM) and adaptive neuro fuzzy inference system (ANFIS) and compared for their efficacy.

Keywords: drilling, regression, ANFIS, RSM, flax-epoxy, FESEM, thrust force

INTRODUCTION

Many industrial and structural applications are increasingly relying on fiber reinforced polymer composites rather than on conventional engineering materials, owing to the advantages they offer, such as high strength, light weight, better corrosion resistance and cost effectiveness.[1-10] In comparison with artificial or synthetic fibers, natural fiber reinforced polymer-based composites hold some exceptional properties, including low price, better thermal and acoustic insulation, design flexibility, high specific strength, biodegradability and low CO_2 emissions, which aid in curbing the effects of climate change and global warming.[11,12] Amongst the most common natural fibers, flax fiber is a highly investigated cellulosic fiber, which is attributed to its outstanding properties, *viz*. better resistance to wear and abrasion, biodegradable nature, high strength to weight ratio, widely available, durable, and with a low cost of production, compared with synthetic fibers.[13]

Knowledge on the free vibrational characteristics of natural fiber composites (NFCs) is imperative for the application of such materials in a dynamic environment. During service, NFCs are subjected to unprecedented cyclic loadings, exerting internal and external vibrations and fatigue in the material structure. In some extreme

cases, this may cause catastrophic failure, provided driving frequency and natural frequency of the NFC material are identical. Sometimes, this may be because of the internal vibration of molecules, resulting in a decrement in service life, unpredicted surface wear, noise damages and fatigue failure. Therefore, experimental techniques should be used to measure the level of vibration endured by the materials.

In recent years, NFC materials have been developed for their use in various automotive parts. However, considering their light weight, they may experience repeated vibration because of road surface irregularities. It is known that the vibrational properties of the materials depend on natural and driving frequencies, and also on their damping factor and, viscoelastic properties (storage modulus, loss modulus). Hence, the vibrational properties of the NFCs and their hybrid composites have been explored. Rajini *et al.*[14] investigated the effect of nanoclay (1, 2, 3, and 5 wt%) and chemical treatments (alkali and silane) on the vibrational property of coconut sheath reinforced hybrid polyester composites. Results showed that enhanced vibrational properties are observed in 3 wt% filled nanoclay hybrid composites. Moreover, modal damping of the composites is highly influenced by both filler addition and chemical pretreatments. Experimentally determined natural frequencies of the composites have been found analogous to analytical results. Etaati *et al.*[15] examined the free vibration property of polypropylene (PP) composites reinforced with different weight fractions of noil hemp fiber (0 to 60 wt%). Amongst the prepared laminates, anhydride-grafted polyethylene octane treated 30 wt% noil hemp fiber reinforced PP composites presented the highest damping capacity. Kumar *et al.*[16] developed hybrid unsaturated polyester composites reinforced with sisal and coconut sheath fiber (as received) using the compression mould process. Their results revealed that, when compared to untreated composites, treated hybrid composites, irrespective of their stacking sequence, exhibited better natural frequency and damping value. Jena *et al.*[17] investigated the damping properties of bamboo-epoxy composites filled with different weight fractions of cenosphere particles. Their experimental results indicated that the composites with higher fiber loading exhibited good natural frequency and damping ratio. Moreover, the vibrational properties completely relied on the cenosphere filler content. Similarly, Uthayakumar *et al.*[18] demonstrated the effect of red mud filler loading (2, 4, 6, and 8 wt%) and particle size (4 µm, 6 µm and 13 µm) on the free vibrational property of the banana fiber reinforced polyester hybrid composites. Higher natural frequency and damping value have been found for 8 wt% red mud filled banana/polyester hybrid composites, containing 6 µm particle size red mud. Interestingly, alkali and silane treatment impacted negatively the vibrational property of hybrid composites containing 8 wt% red mud filler of 4 µm particle size.

Bennet *et al.*[19] reported on vibrational properties of *Sansevieria cylindrica*/coconut sheath polyester hybrid composites. Their study clearly indicated that chemically treated (alkali and silane) hybrid composites showed improved mechanical and vibrational properties compared to single fiber composites. Arulmurugan and Venkateshwaran[20] in their study incorporated the optimum nanoclay amount into jute/polyester composites to study the combined effect of fiber and filler content on the vibrational properties of the hybrid composites. Vibrational results showed that 15 wt% jute reinforced polyester composites with 5 wt% nanoclay displayed superior natural frequency and damping factor. Moreover, experimental results have shown good agreement with theoretical analysis. Arvinda Pandian and Siddhi Jailani[21] examined viscoelastic and free vibrational characteristics of jute/linen reinforced epoxy hybrid composites. Composites with equal proportion of jute and linen (10 wt%) exhibited superior mechanical, natural frequency (27 Hz) and damping coefficient (0.035) amongst the prepared hybrid laminates. Senthilkumar *et al.*[22] reported that the natural frequency of pineapple leaf fiber (PALF) reinforced polyester composites increases with an increase in fiber loading, whereas damping factor decreases, and further suggested 45 wt% of PALF for making structural components. Sumesh *et al.*[23] assessed the vibrational properties of the sisal, banana, and coir reinforced epoxy hybrid composites filled with different weight fractions of nano alumina powder derived from *Muntingia calabura* leaf. Results revealed that the addition of green nano powder substantially enhanced the natural frequency and damping factor of composites containing 35 wt% of fiber reinforcement. Kumar *et al*.[24] for the first time evaluated the free vibrational characteristics of the *Phoenix* sp. fiber reinforced polyester composites. These novel

hybrid composites were fabricated by varying fiber length, fiber content (vol.), concentration of alkali, and weight fraction of filler (nanoclay) using the compression mould method. Modal analysis showed that the optimum value of fiber length and volume fraction responsible for better vibrational properties is 40 mm and 40% respectively. Moreover, up to 242% improvement in terms of natural frequency can be achieved for epoxy resin by employing the aforesaid reinforcements. Chandrasekar *et al.*[25] concluded in their investigation that fiber inter-ply orientation had significantly affected the mechanical and free vibrational properties of banana fiber reinforced polyester composites. Rajamurugan *et al.*[26] in their research report concluded that the addition of 5 wt% of $BaSO_4$ filler to *Aloe vera*/hemp/flax woven epoxy hybrid composites had improved natural frequency and damping values in all four modes of analyses. Such a tremendous enhancement may have been due to the increase in the stiffness of the composites as imparted by the added ($BaSO_4$) filler.

Recently, many well-known European car manufacturers have shown interest in employing NFCs for automotive interior and exterior parts.[13,27] In a view of expansion of NFCs usage in both structural and non-structural applications, these NFCs produced by primary processes closer to near net shape products still have to undergo secondary machining operations to attain the dimensional requirements or constraints. Of the various machining operations, traditional drilling is the most popular and most sought-after process for producing secondary operations, especially for making most economical holes. However, drilling of NFCs has been a quite complicated task as the material system is an anisotropic and non-homogenous structure, reinforced with hard fibers having high abrasiveness.[28,29] Because of this, during the drilling operation, friction between the drill tool and the fiber results in high temperature causing matrix to soften, eventually paves for fiber pull-out, and thermal degradation. Also, because the difficulty of tool penetration into hard reinforcement results in high thrust force and torque, this causes delamination, uncut fiber, spalling and hole shrinkage.[30] Among those noteworthy problems, delamination as a result of high thrust force and torque, and surface roughness of the drilled hole play a critical role, directly reflecting on the quality of the holes and their accuracy as well.

The manufacturing process aims to produce good quality products with minimum effort, and the only way to achieve this is by means of experiments. It is known that the drilling quality of NFCs is dependent on several factors, as described previously.[11,13,26,29] Therefore, it takes many trials to find the optimal solutions, which eventually consumes time and incurs high costs. Thus, for minimizing the number of tests or trials, the statistical approach can be employed for planning and conducting the experiments, allowing analyzing of the data for minimizing errors. Moreover, building a predictive model based on empirical information to predict the machining performance is essential, and it is the need of the hour to consider for producing high-quality holes. Generally, the regression model is implemented to draw relationships between output responses of the drilling with input control parameters. Mata *et al.*[30] proved that predicted results obtained for carbon reinforced PEEK composites are almost similar to experimental ones, and hence conveyed that the regression model was effective. Onwubolu and Kumar[31] reported that the response surface methodology (RSM) model developed for drilling aluminium alloy was useful not only for predicting optimal conditions for achieving quality holes, but also for process optimization. Jayabal *et al.*[32] applied the regression model for drilling polyester hybrid composites to predict output responses, namely, thrust force, torque, and wear of tools. The study reported that predicted results are in line with the experimental ones, and so the developed model was significant. Valarmathi *et al.*[33] investigated the surface roughness quality of drilled holes using the RSM approach in particle board composites. The developed regression model was found to be effective in predicting the experimental results. Amongst the developed models, the quadratic one was also found significant. Karthik and Sampath[34] developed an experimental regression model that proved able to predicting the thrust force in drilling cotton/bamboo hybrid epoxy composites. Anjinappa *et al.*[35] implemented RSM modelling in studying the effect of drilling parameters on the evaluation of thrust force in sheep horn particle reinforced epoxy composites. The outcome of their study revealed that feed rate and spindle speed were the most significant parameters influencing the output response – thrust force. The developed regression model under the central composite design, with an R^2 value of 0.926,

proved adequate. Kumar *et al*.[36] used the RSM model for optimizing the abrasive water jet machining parameters in drilling Inconel 718 nickel base alloy. Their results showed that predicted surface roughness values were close to experimental results, and a confirmation test validated the capability of the developed RSM model. Rajamurugan *et al.*[37] studied drilling of coir/polyester composites using a multifaceted drill bit. Input parameters, such as sample thickness, drill diameter, feed and spindle speed, were chosen against the output response delamination. Results confirmed that the feed rate was the most influential parameter in increasing delamination. The quadratic RSM model developed was suitable for predicting the drilling output response, with an R^2 value greater than 0.96.

In the last decade, several researchers have investigated the ANFIS (Adaptive Neuro-Fuzzy Inference system) predictive model, which is basically an integration of the properties of fuzzy logic and artificial neural networks.[38] ANFIS overcomes the demerits associated with the latter one, and hence, it is applicable in solving numerous practical problems.[39] As far as drilling of materials is concerned, the ANFIS based model may be applied to predict desired output responses like thrust force, surface roughness, life of the tool, delamination factor and torque. Azmi[40] studied the tool wear and feed force during the milling of glass fiber polymer composites with the help of the ANFIS model. According to their results, the predicting capability of the model was found superior within the confidence level. Manikandan *et al.*[41] applied the ANFIS technique in the wire electrical discharge machining process for predicting the desired performance (material removal rate, surface roughness) in machining LM6/SiC/dunite hybrid metal matrix composites. Ozden *et al.*[42] reported about the prediction of the cutting forces generated during the turning operation of PEEK composites using the ANFIS method. Experimental and predicted results showed good accuracy and proved the model's efficacy in predicting cutting force. Kumaran *et al.*[43] reported the usefulness of the ANFIS model for predicting the experimental values of surface roughness in abrasive waterjet machining of carbon fiber reinforced plastics. Marani *et al.*[44] explained the effect of various parameters on machinability of Al–20 Mg_2Si metal matrix composites. The ANFIS model was successfully developed for predicting the surface roughness and cutting force, the model was found effective and it minimized the experiment repetition.

Our literature survey revealed that ANFIS has not been implemented so far specifically for assessing the drilling performance of flax/epoxy (F-Ep) composites. Hence, this research work aimed to achieve high-quality holes in F-Ep composites using regression models to predict the optimal parameters. The prediction of the thrust force was performed using ANFIS and RSM models, and the results were then compared with experimental ones to validate the suitability of the models.

EXPERIMENTAL

Materials

The flax/epoxy composites (F-Ep) studied in this current investigation contained plain basket woven flax fabric used as reinforcement. The flax fiber surface was treated with trimethoxymethylsilane coupling agent to enhance the interfacial bonding between the matrix and the fiber. Epoxy resin (VBR 8912 grade), with room temperature curing hardener (VBR1209), was employed as matrix material. The silane treated F-Ep composites were prepared by the compression moulding technique, as described in our previous studies.[1,45] The F-Ep composites were prepared by curing at room temperature (27 °C) for 24 hours under constant pressure of 250 psi (17.25 bar). The details on the formulation and denotation of the F-Ep composites are shown in Table 1.

Free vibration test

Figure 1 shows the schematic representation of the FVT setup, where F-Ep composite specimens were tested to comprehend their dynamic behavior characteristics. The dimension of the composite specimens for the FVT test should be: 200 mm×20 mm×3.2 mm. For the tests, one end of the F-Ep specimen was clamped and the other end was allowed to deflect, as illustrated in Figure 1. F-Ep composite specimens were excited by the impact hammer (Kistler model 9722A500) at 10 different points, due to which the accelerometer generated displacement signals, which were recorded using a data acquisition system (DEWE 43, Dewetron Corp., Austria), stored in the computer system. A minimum of three F-Ep specimens were tested for each composition, and the average value was considered for computing the damping ratio and natural frequency. The logarithmic decrement (δ) of the F-Ep samples was determined by using Equation (1):

$$\delta = \frac{1}{n}\ln\left(\frac{X_o}{X_n}\right) \quad (1)$$

where X_o and X_n indicate the initial and n^{th} amplitude of the vibration, respectively, and n denotes the number of cycles.

Figure 2 shows the half power band width curve, which has been employed to determine the damping factor (ς) of the F-Ep composites using Equation (2):

Damping factor (ς) = $\Delta\omega/2\omega_n$ (2)

where $\Delta\omega = \omega_{a2} - \omega_{a1}$; ω_{a1} and ω_{a2} are the corresponding frequencies obtained for the points a_1 and a_2 on the curve, as shown in Figure 2; ω_n and ς are the natural frequency and damping factor of the F-Ep composite sample, respectively.

Table 1
Composition of F-Ep composites

Composite code	Weight fraction of constituents (wt%)		Layers of fabric used	Density of composites (g/cc)		Void (%)
	Epoxy resin	Flax fiber		Theoretical	Experimental	
Neat epoxy	100	0	-	1.22	1.16	4.91
25F-Ep	75	25	4	1.24	1.19	4.03
35F-Ep	65	35	4	1.27	1.21	4.73
45F-Ep	55	45	4	1.34	1.30	2.98

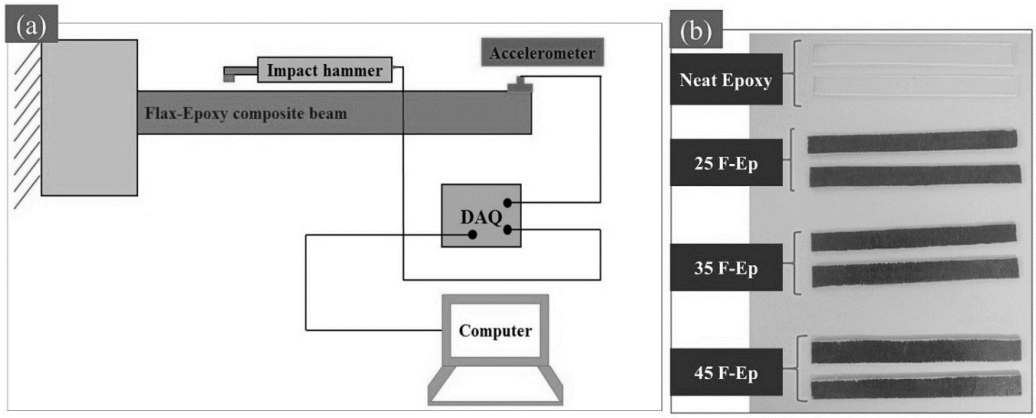

Figure 1: a) Schematic representation of the free vibration test setup (FVT), b) FVT specimens

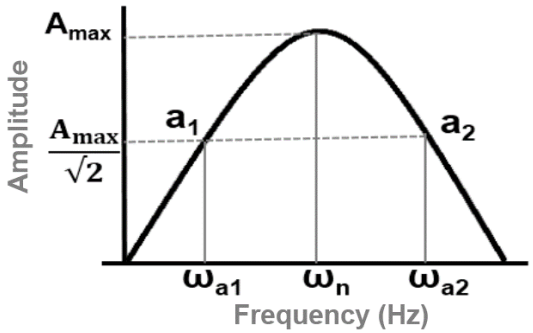

Figure 2: Half power band width curve[12]

Drilling setup

Drilling was performed on the 45F-Ep composite in a vertical CNC machine, using a 6 mm HSS twist drill diameter. Spindle speed (1000, 2000, and 3000 rpm), feed rate (25, 50, and 70 mm/min) and drill point angle (90°, 118° and 130°) were the input parameters considered, and the output response was thrust force, as it directly affects the delamination damages occurring around the holes. Thus, by finding out the suitable combinations of the input parameters, thrust force can be minimized, and thus, the delamination. Figure 3 depicts different drill point geometries used for drilling the F-Ep composite.

In the initial setup, the F-Ep specimen was firmly placed on the force dynamometer (Kistler) with the help of the fixture. The responses, such as thrust force signals, were recorded through the dynamometer and were further processed through the data acquisition system for concluding their numerical values. The

delamination factor of the F-Ep composite was determined using Equation (3):

$$d_f = D_{max} / D_{nominal} \quad (3)$$

where d_f denotes the delamination factor; D_{max} and $D_{nominal}$ represent the maximum diameter and nominal diameter of the drilled hole, respectively, as indicated in Figure 4.

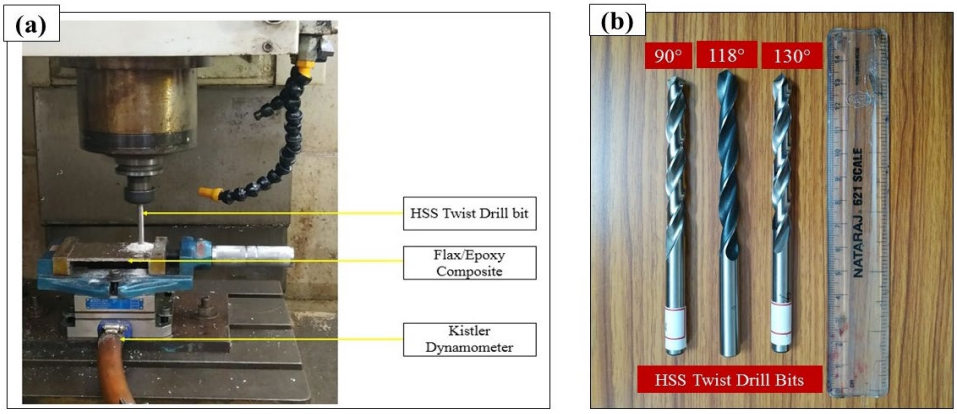

Figure 3: a) Experimental drilling set up, b) Different geometry of HSS drill bit used

Table 2
Control factors and their levels

Control factors	Levels			Units
	I	II	III	
Spindle speed (A)	1000	2000	3000	rpm
Feed rate (B)	25	55	75	mm/min
Drill point angle (C)	90	118	130	° (degree)

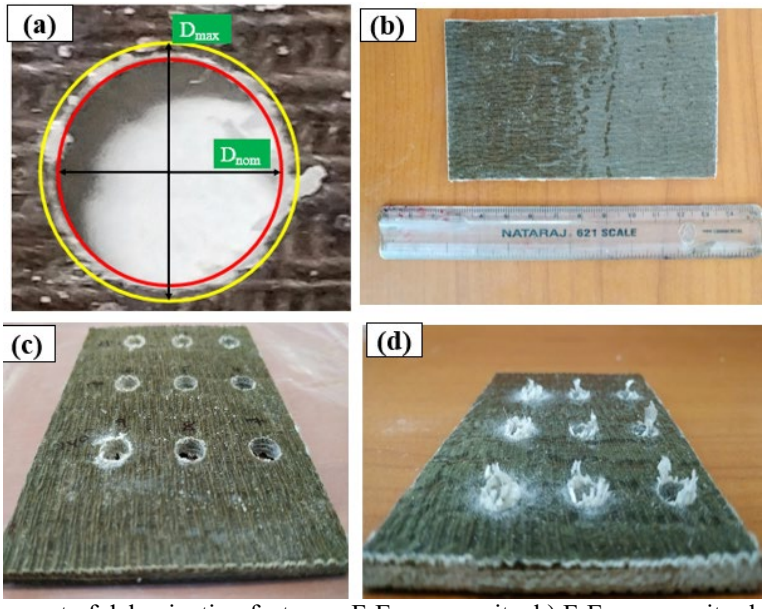

Figure 4: a) Measurement of delamination factor on F-Ep composite, b) F-Ep composites before drilling holes, c) Peel-up delamination, d) Push-out delamination[46]

Design of Experiments (DOEs)

Taguchi orthogonal arrays (OAs) are employed to analyse the complete process parameter by performing only a few sets of experiments. The main intention of the Taguchi design of experiment technique is to avoid the repeated tests, which eventually saves time, material and cost. The Taguchi based design of experiment approach is widely employed by researchers in the study of drilling behavior of the materials. In this study, by this approach, all possible combinations of factors were experimentally explored. The Taguchi methodology on experimentation offers an orderly way to collect, analyse and interpret data to meet the objectives of the study. By application of

DOEs, the maximum amount of the information for the amount of experimentation can be obtained. This is accomplished by running the experiments with combinations of the variables to be investigated, as suggested in the design layout. The crucial moment of the experiments lies in the selection of parameters affecting the process. The Taguchi method creates standard OAs to contemplate the effect of several factors on the target value and defines the plan of experiments. In this study, experimental design L_{27} OA was selected, with three factors: spindle speed, feed rate, and drill point angle, and each of their three levels are shown in Table 2. During drilling, the generated thrust force, which is the main response of the study, was recorded (Table 3) and the process parameters with their interaction effect were analysed.

Table 3
Drilling results of F-Ep composites

Trial No	Levels of factors			Thrust force (N)
	A	B	C	
1	1000	25	90	50.72
2	1000	25	118	43.44
3	1000	25	135	37.08
4	1000	50	90	46.22
5	1000	50	118	42.66
6	1000	50	135	32.04
7	1000	75	90	41.66
8	1000	75	118	33.42
9	1000	75	135	28.75
10	2000	25	90	50.75
11	2000	25	118	36.80
12	2000	25	135	31.52
13	2000	50	90	26.91
14	2000	50	118	33.54
15	2000	50	135	30.95
16	2000	75	90	23.25
17	2000	75	118	30.23
18	2000	75	135	24.25
19	3000	25	90	20.86
20	3000	25	118	36.82
21	3000	25	135	31.12
22	3000	50	90	26.65
23	3000	50	118	22.75
24	3000	50	135	28.36
25	3000	75	90	26.17
26	3000	75	118	19.66
27	3000	75	135	25.56

RSM and ANFIS models

In this study, RSM and ANFIS modeling techniques were employed and their respective models were developed by using Design Expert and MATLAB software. RSM is applied to establish the relationship among the various input parameters and explores the effect of these process parameters on the selected responses, (*i.e.* thrust force in this study). In addition, quantitative connection between reactions and the information factors can be analysed by implementing the RSM modeling technique.

The relationship between the control parameters of drilling F-Ep composites and the response (thrust force) is shown in Equation (4):

$$f_u = \psi(x_{1u,} x_{2u,} x_{3u,} \ldots x_{k\,u}) + \varepsilon_u \quad (4)$$

where u=1,2,3,…k and k represents factorial experiment number; x_{iu} denotes the level of the i^{th} factor in the u^{th} experiment. The function ψ is called the response surface. The residual ε_u measures the experimental error in the corresponding u^{th} observation.

The second order polynomial equation, that is, quadratic response surface has two variables and is given in Equation (5):

$$f_u = \beta_0 + \beta_1 x_{1u} + \beta_2 x_{2u} + \beta_{11} x_{1u}^2 + \beta_{22} x_{2u}^2 + \beta_{12} x_{1u} x_{2u} + \varepsilon_u$$

where $\beta_{0,}$ $\beta_{1,}$ β_2 ….. are the regression coefficient of the input variable (x).

The quadratic model indicated in Equation (5) is created for expecting the approximation of the output variable by the values received through experiments. Further, its efficacy is validated by ANOVA. Finally,

model fitness is checked by the coefficient of determination (R^2) value.

ANFIS is integrated with neural network and a fuzzy logic concept.[24] ANFIS is very fast, owing to the hybrid learning procedures it uses with multilayer feedforward network. Multi-layers of nodes are interconnected using directional links. Error in the system can be brought down by changing the input parameters.[39] The magnitude of each input control factor in the ANFIS system is graphically represented as a curve, which is defined by the membership function (MF). There are many membership functions are available for relating each of the input factors with output response variables. In this study, 'gbellmf,' 'gaussmf,' and 'gauss2mf,' types of Gaussian membership functions are used. In ANFIS, training is performed for various iterations and 27 fuzzy rules are generated based on the input parameters. Thus, the proposed system converged with minimum root mean square error value 0.00345 at 100th epochs. ANFIS parameters and their respective membership functions are given in Table 4.

There are mainly two types of fuzzy inference systems (FIS): Mamdani FIS and Sugeno FIS. For the present study, the latter technique is employed and its functioning principle and architecture is shown in Figures 5 and 6, respectively. Validation of the drill input parameters with the process involved in Sugeno FIS is depicted in Figures 7 and 8, respectively. The root mean square error (RMSE) and mean absolute error (MAE) of the predicted and experimental values can be computed using Equations (6) and (7) respectively:

$$RMSE = \sqrt{\frac{\sum (j-k)^2}{m}} \quad (6)$$

$$MAE = \frac{\sum |j-k|}{m} \quad (7)$$

where m, j and k are number of patterns, set of actual and predicted output, respectively.

The coefficient of determination (R^2) was determined for understanding the effectiveness of the mathematical model used and its value generally ranges from 0 to 1. Equation (8) was utilized for calculating the R^2 value, which gives an insight into the relationship between one term's performance and its prediction on the performance of another term:

$$R^2 = 1 - \frac{\sum (j-k)^2}{\sum (j-\bar{k})^2} \quad (8)$$

where $\bar{k}$ is the mean of the predicted output.

The accuracy of the performance factors calculated is in 10^{-4}. The model with the minimum average checking error is preferred, which gives good results.

Table 4
ANFIS information of membership function for drilling F-Ep composites

Sl. No	Parameters	Membership functions		
		gbellmf	gaussmf	gauss2mf
1	Number of nodes	222	222	222
2	Linear	108	108	108
3	Non-linear	162	165	168
4	Total number of parameters	270	273	276
5	Number of fuzzy rules	27	27	27

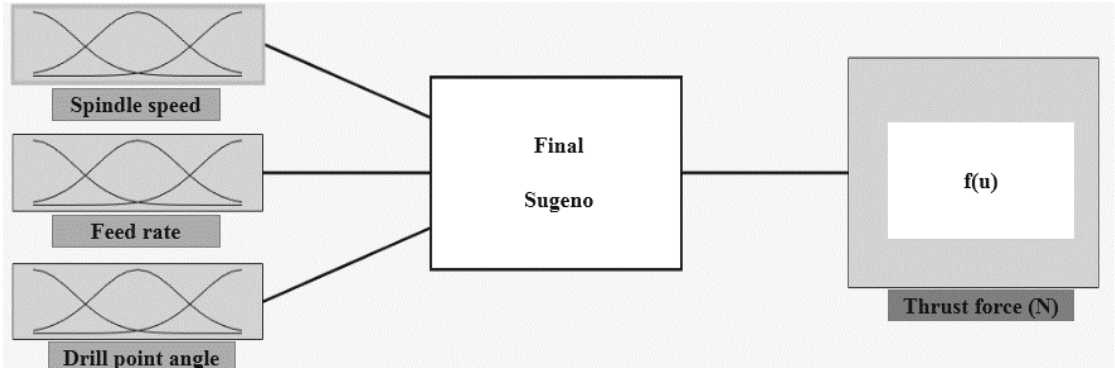

Figure 5: Sugeno model with three inputs

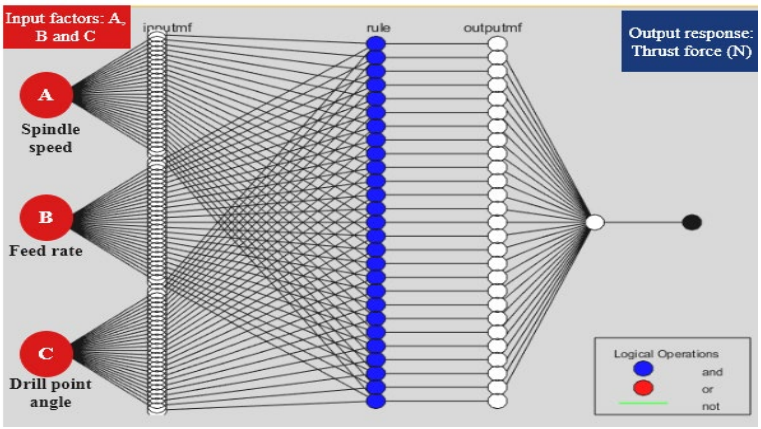

Figure 6: ANFIS architecture employed for drilling F-Ep composites

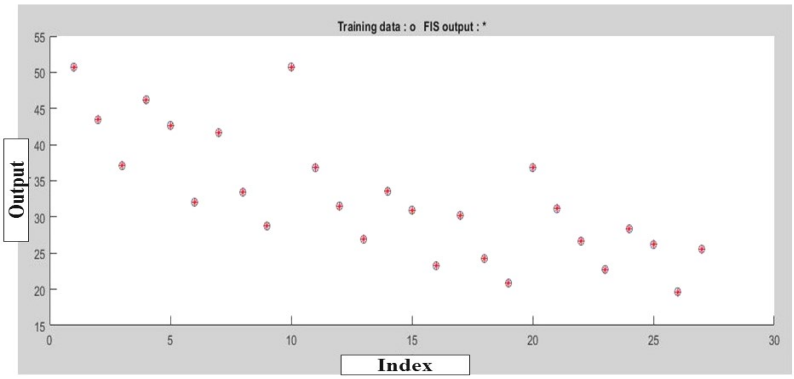

Figure 7: Validation of input drill parameters with Sugeno model in MATLAB (R2017a)

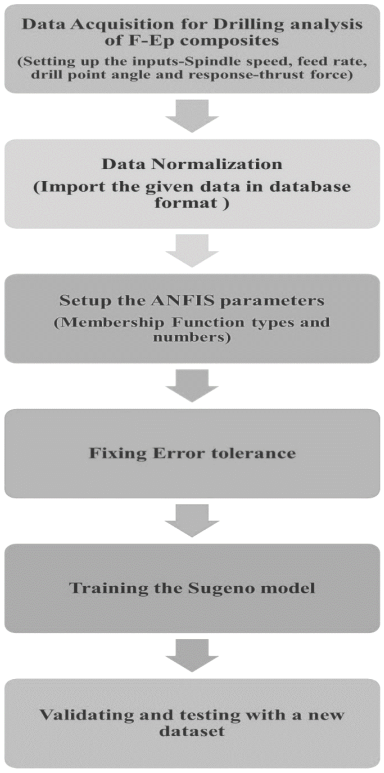

Figure 8: Steps involved in training of input drill parameters with Sugeno model

RESULTS AND DISCUSSION

Vibrational properties of F-Ep composites

In fact, finding these vibrational properties is fundamentally needed in the design process to prevent resonance condition. Besides, beams have infinite degrees of freedom and so enormous natural frequencies and mode shapes. The first mode of the natural frequency is considered in the current investigation and it has been extracted using the frequency response function curves generated in DEWEsoft 7.3 software. A sample plot generated by the system is shown in Figure 9, for the 35F-Ep composite. The natural frequency of the silane treated F-Ep composites at varying flax fiber content is shown in Figure 10 and detailed experimental results of the free vibration test are presented in Table 5. From the plot, it is understood that an increase in the fiber content increases the natural frequency of the composites. This is attributed to the good interfacial bonding between reinforcement and matrix, as a result of the chemical treatment. Amongst the fabricated F-Ep composites, 45F-Ep has a higher natural frequency (29.6 Hz), owing to its increased modulus due to strong fiber-matrix adhesion. These findings are in accordance with earlier reports.[17,47]

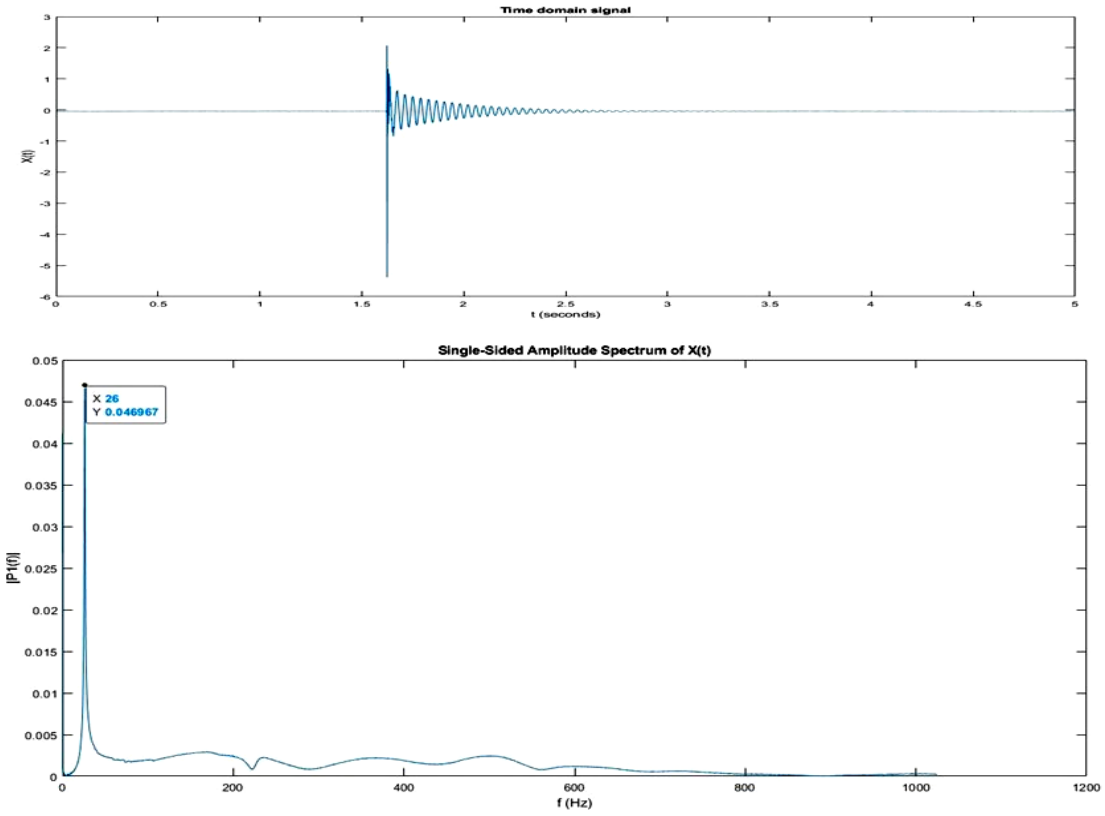

Figure 9: Frequency response function curve of 35F-Ep composites

Table 5
Natural frequencies and damping ratio of F-Ep laminates

Composites	log decrement (δ)	Damping ratio (ς)	Natural frequency mode I (Hz)	
			Experimental value	Theoretical value
Neat epoxy	0.1198	0.0180	19.2	19.16
25F-Ep	0.0811	0.0124	23.4	26.04
35F-Ep	0.1344	0.0201	26.2	28.60
45F-Ep	0.1680	0.0247	29.6	31.20

Natural frequency of the composites depends on various factors, such as stiffness of the fiber, orientation of the fabric, weaving pattern, types of chemical treatment performed *etc*. According to

the findings of Rajesh *et al.*,[48] basket woven fabric reinforced polyester composites exhibited higher natural frequency compared to the non-basket (other weaving pattern) composites. Because basket weave provides low crimp between warp and weft directions, and also these patterns are symmetric in nature. A similar explanation can be applicable for the present investigation as well, since the flax fiber used as reinforcement in the epoxy represents plain irregular basket woven fabric. Table 5 clearly shows that 45F-Ep composites exhibited 45.5% improvement of natural frequency compared to the neat epoxy resin, because the modulus of the composites is improved after reinforcement. Theoretical results of the natural frequency for mode I were obtained by the Euler-Bernoulli beam theory, using Equation (9):

$$\omega_I = 1.875^2 \sqrt{\left[\frac{EI}{\rho A L_C{}^4}\right]} \quad (9)$$

where E is the Young's modulus of the composites, I is the moment of inertia (mm^4), A is the cross sectional area of the composites, ρ is the density of the composites (kg/mm^3), and L_C is the length of the composite (mm).

Figure 10 shows that experimental and theoretical frequencies of the silane treated F-Ep composites are in good agreement to each other.

The dynamic behavior of the fiber reinforced polymer composites can be interrelated with the damping factor, and thus it is very important to understand the damping property of the composites. Furthermore, a balance between viscous and elastic phases in the polymer structure can be established by knowing its damping property. The damping ratio of the silane treated F-Ep for varying weight fraction of fiber is presented in Figure 11. From the plot, it can be observed that the damping ratio increases with an increase in the fiber content. This is attributed to the strong energy dissipation through the fiber-matrix interface. Moreover, an increase in the fiber content enhances the rigidity of the composites.[17,47] Amongst the fiber composites, the 45F-Ep composite showed the highest damping ratio (0.0247).

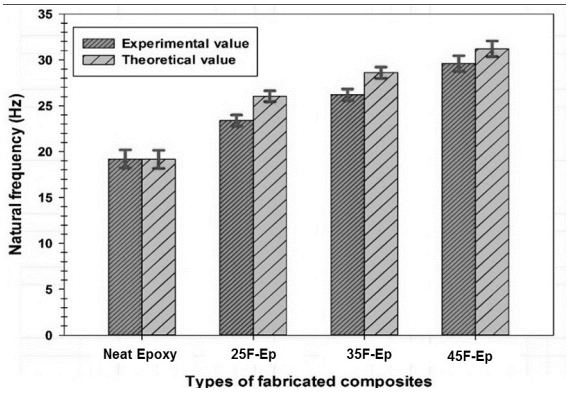

Figure 10: Experimental and theoretical natural frequency (mode I) of neat epoxy and silane treated F-Ep composites

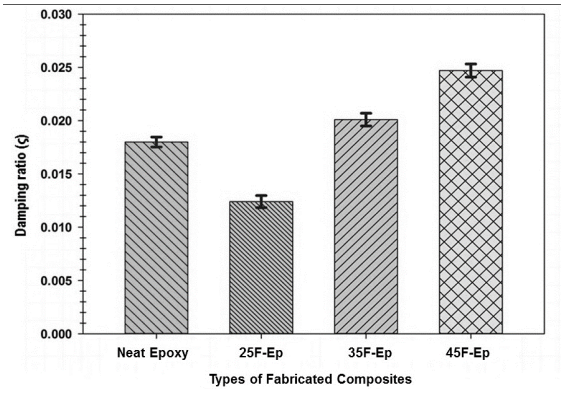

Figure 11: Damping ratio of neat epoxy and F-Ep composites

Drilling characteristics of F-Ep composites

Before converting the composite materials to useable products, they have to undergo various stages of machining operations. In this process, achieving of high surface quality with less damages is very vital and it can be taken care of, if machining conditions are wisely selected.[49] In the present work, the drilling operation was performed on the F-Ep composites using varying input factors: spindle speeds, feed rates and drill point angles, which are in accordance with the Taguchi L_{27} OA, and varied at three levels, totally leading to 27 combinations. In the first nine trials, spindle speed (A) was maintained at 1000 rpm, for the next nine trials it was increased to 2000 rpm, and to 3000 rpm for the remaining nine trials. The feed rate (B) was varied after every three trails from 25 to 50, and then to 75 mm/min. Drill point angles (C) differed in each trial, as indicated in Table 3, and it is clearly seen that the thrust force value obtained ranged from 19.66 to 50.75 N. From the table, it is observed that the increment in the thrust force values is due to the increase in the drill point angle. Hence, lower levels of point angle drill bits are preferred for F-Ep composites. Also, it is observed that thrust force decreases with increasing spindle speed and

feed rate. Hence, their lower levels are preferable for drilling F-Ep composites.

From the experimental investigation, results revealed that all three factors and their various combination have a significant impact on the thrust force generated during drilling of F-Ep composites. It is clear that F-Ep composites drilled using a twist drill with a lower drill point angle at higher feed rate and spindle speed combination would reduce the thrust force generation, and thus the delamination of the composites. After conducting the experiments, experimental values were utilized to build the RSM and ANFIS models in order to analyse their predicting capability and compared to settle the best modelling approach. ANOVA was employed to analyse the drilling conditions, which minimize the thrust force. Namely three RSM models: linear, 2FI, and quadratic, were developed and their efficacy in forecasting the thrust force values was studied. Table 6 and Table 7 show the summary of the RSM model and its equation generated using the quadratic method, respectively, and it is clear that the R^2 value of the quadratic model is superior to that of the other two models. Figure 12 presents the normal probability plot and Figure 13 depicts the relationship between the predicted and actual values of the thrust force. It is evident from the plots that thrust force values have been distributed normally and expected values are closer to the real ones and thus the model is beneficial.

Table 6
Summary of the RSM models

Source	Standard deviation	R^2	Adjusted R^2	Predicted R^2	PRESS
Linear	5.44	0.6536	0.6085	0.498	985.98
2FI	4.72	0.773	0.7049	0.5086	965.12 (suggested)
Quadratic	5	0.7837	0.6692	0.3762	1225.03

Table 7
RSM model for thrust force

Response	Model expression	R^2
Thrust force (N)	88.83-0.03365*A-0.517*B+0.1465*C+3.335E-05*A*B+1.88E-04*A*C+1.29E-03*B*C+9.76E-07*A^2+1.063E-03*B^2-3.09E-03*C^2	78.37%

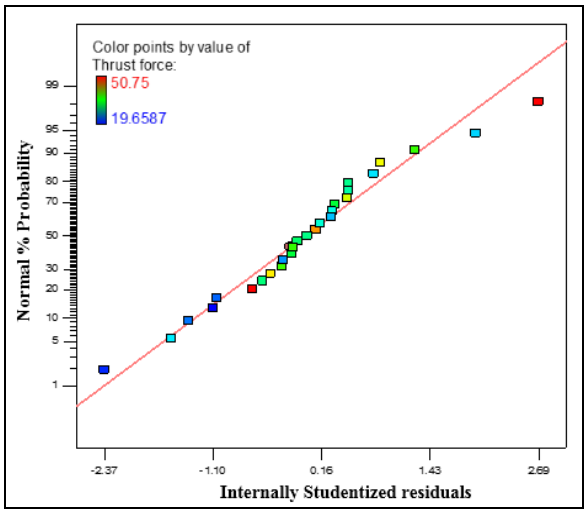

Figure 12: Normal probability graph

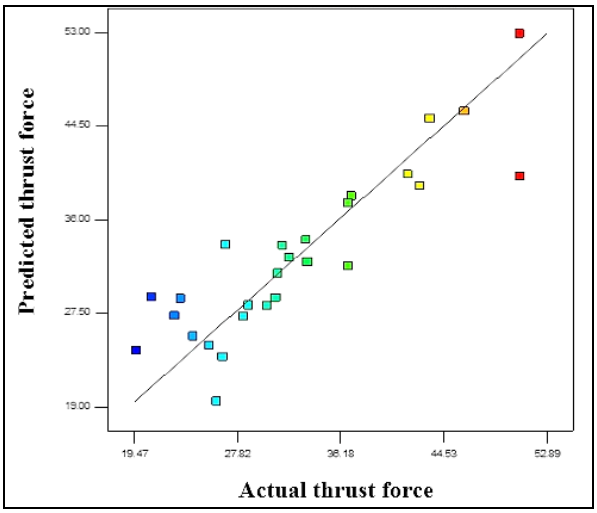

Figure 13: Correlation graph for thrust force

The RSM graphs are presented in Figure 14, mainly to visualize the response surface. In the surface plot, the interaction effect of two factors on the thrust force (response) is considered by maintaining the third factor constant. From Figure 14, it is observed that the thrust force value is lower at higher spindle speed and *vice-versa*. Thrust force generated during the drilling of F-Ep composites decreased when the spindle speed increased from 1000 to 3000 rpm. Furthermore, it

was also noted that the thrust force value was high when the holes in the F-Ep composites were produced at a lower feed rate. Thrust force decreases as the feed rate is increased from 25 to 75 mm/min. From the plot, it is understood that low spindle speed and feed rate would be the best combination for producing lower thrust force during drilling of F-Ep composites, and so better quality holes can be produced by preventing delamination.

From the plot, it was also noted that the thrust force value increases with an increase in the drill point angle and decreases with an increase in spindle speed. Hence, smaller drill point angle and spindle speed combinations are appropriate conditions for a better output response. Figure 14 reveals that F-Ep composites drilled using a low drill point angle at the minimum feed rate would be the best combination to reduce the thrust force generation.

Modeling of the thrust force has been performed using the ANFIS tool. Typical ANFIS results of the current study are detailed in Table 8. From the table, it is evident that the ANFIS model trained under 'gbellmf" with 100 epochs gave the minimum error in predicting the response values (thrust force), compared to the other two membership functions. Hence, it is the most suitable for modeling the input factors in drilling F-Ep composites. Figure 15 depicts the ANFIS surface plots of thrust force obtained for F-Ep composites. The graphs clearly explain the interaction effects of spindle speed and feed rate, feed rate and drill point angle, and speed and drill point angle on the output response thrust force. From the plots, it can be deduced that the thrust force response is effective when drilling on the F-Ep composite is performed at high speed and feed rate using a drill point angle at a smaller scale.

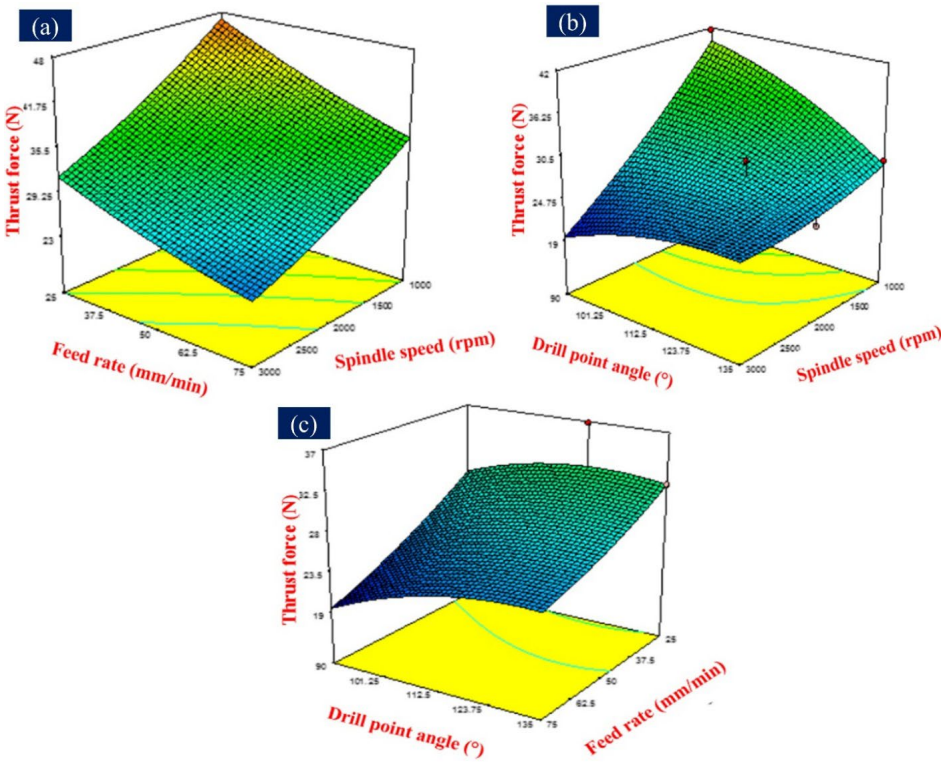

Figure 14: RSM graphs for response thrust force

Table 8
Information of ANFIS model chosen for drilling F-Ep composites

Model parameters	Membership functions		
Chosen membership function	gbellmf	gaussmf	gauss2mf
No. of epochs	100	100	100
Error (%)	0.0345856	0.0375823	0.0356744

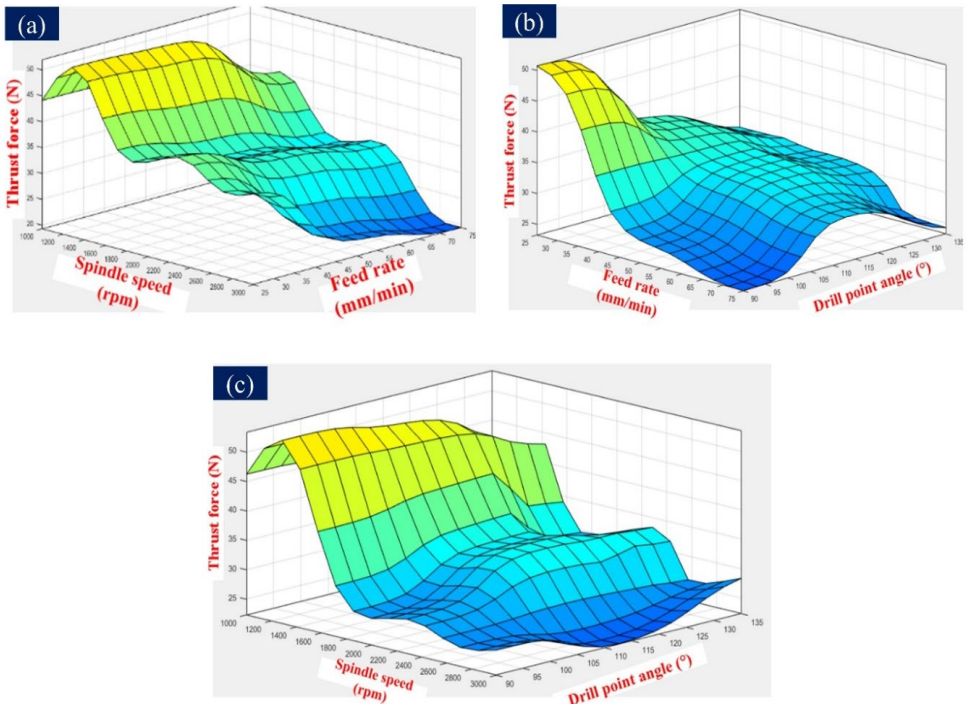

Figure 15: ANFIS three dimensional graphs for the response thrust force

Table 9
ANOVA for thrust force in drilling F-Ep composites

Source	DF	Seq SS	Adj SS	Adj MS	F	P
Regression model	9	1539.17	1539.17	171.02	6.84	0.0004 (significant)
Spindle speed (A)	1	1.27	1.27	1.27	0.051	0.8241
Feed rate (B)	1	0.15	0.15	0.15	6.07E-03	0.9388
Drill point angle (C)	1	15.37	15.37	15.37	0.61	0.4437
AB	1	8.33	8.33	8.33	0.33	0.5712
AC	1	219.66	219.66	219.66	8.79	0.0087
BC	1	6.41	6.41	6.41	0.26	0.619
A^2	1	5.71	5.71	5.71	0.23	0.6386
B^2	1	2.63	2.63	2.63	0.11	0.7497
C^2	1	12.72	12.72	12.72	0.51	0.4853
Residual error	17	424.77		24.99		
Total	26	1963.94				

The significant factors affecting the thrust force response were evaluated by means of ANOVA and are presented in Table 9. The F-value of 6.8 and R^2 value of 78.37 reveal that the model is significant. ANOVA results showed that C, C^2 and AC are significant, influencing the thrust force response. The combined effect of different parameters was analysed by the interaction effect plots. The interaction plots are depicted in Figure 16. It is observed that thrust force is minimum at high spindle speed and smaller drill point angle combinations. At high speed, heat generation is highly significant due to the friction between the drill bit and the reinforcement element of the composite material. The developed heat is sufficient to melt the polymer and softened polymer helps in easing removal, resulting in the generation of lower thrust forces when drilling holes. However, when the F-Ep composite is drilled at lower spindle speed, it experiences low strain rates and consumes longer machining time, which leads to higher drilling forces, in contrast to the high-speed drilling condition. From Figure 16, it is observed that the following combinations: smaller drill point angle and larger feeds, and larger feeds with high spindle speed – show decreased thrust force value. So, the thrust force can be minimized when F-Ep composites are drilled by keeping the

spindle speed and feed rate in the higher level and the drill point angle at a smaller level.

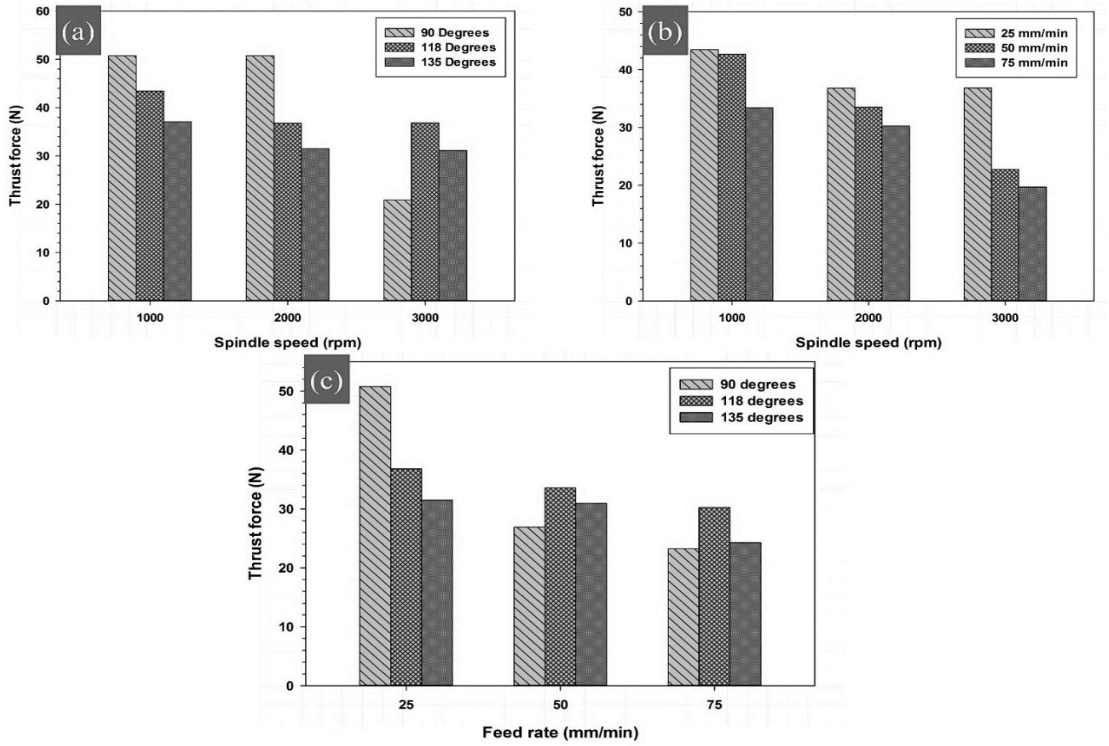

Figure 16: Interaction plots of the desired response with input parameters

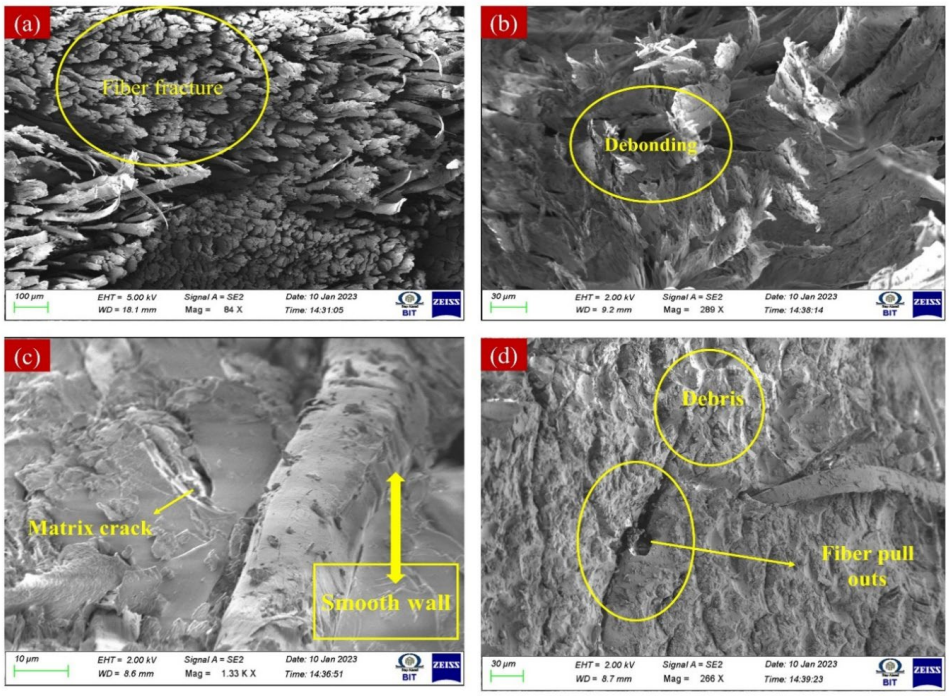

Figure 17: FESEM images of the drilled surface of F-Ep composites

FESEM images (Fig. 17 (a-c)) of drilled holes in F-Ep composites show fiber fracture, debonding, fiber pull-outs, drilled debris and matrix crack in the proximity of the fiber region. Figure 17 (a) clearly reveals that the drilled surface is quite rough, as it is evident due to the projections of the fibers after heavy fracture, owing to the high thrust force developed during the drilling action. At magnifications of 290X and 1300X, it is evident that debonding of the fiber

from the matrix is not prominent, which is attributed to the strong bonding between the fiber and the matrix as a result of the silane treatment. Furthermore, the drilled hole exhibits a smooth matrix surface, with less delamination, when F-Ep was drilled at high spindle speed with high feed rate using a low drill point angle tool, as indicated in Figure 17 (c). This may be due to the softening of the epoxy matrix as a result of the high temperature generated between the drill bit and the reinforcement member. In this case, if the F-Ep composite is not impregnated uniformly by epoxy resin, brittleness of the material could be evident, leading to more fiber fracture around the drilled holes and resulting in higher roughness, as indicated in Figure 17 (a). From the FESEM analysis, it can be deduced that heavy fiber breakages and protrusion in the drilled holes of F-Ep composites are mainly attributed to the high thrust force developed during drilling. Thus, proper selection of drilling parameters is vital for producing high quality drilled holes in F-Ep composite materials.

In this work, two types of modeling techniques were employed and their effectiveness is compared in Table 10. The R^2 values of RSM and ANFIS were found to be 0.783 and 0.988, respectively, which indicates the ANFIS model is superior to RSM. A comparison of the thrust force values obtained experimentally, and through ANFIS and RSM is depicted in Figure 18. It clearly conveys the predicting effectiveness of the ANIFS and RSM models. The developed models were implemented and analysed by performing confirmation tests. The drilling conditions for conducting confirmation tests were selected based on the factors and levels considered in this work. The values shown in Table 11 explain the predicting ability of the developed models. Thus, these models can predict the thrust force value generated in the F-Ep composites for the ranges of drilling parameters considered. The confirmation test revealed that the experimentally obtained thrust force values are in close agreement with those predicted by the ANFIS model, followed by RSM, as illustrated in Figure 19.

Table 10
R-Sq values of RSM and ANFIS models for F-Ep composites

Response	R-Sq values	
	RSM model	ANFIS model
Thrust force (N)	0.783	0.988

Table 11
Confirmation experiments for validating the values predicted by RSM and ANFIS models

Expt. No	Model employed	Spindle speed (rpm)	Feed rate (mm/min)	Drill point angle (degrees)	Thrust force (N)
	Experimental	1500	60	90	42.78
1	RSM	1500	60	90	34.65
	ANFIS	1500	60	90	43.08
	Experimental	1500	60	118	41.88
2	RSM	1500	60	118	34.21
	ANFIS	1500	60	118	42.58
	Experimental	1500	60	130	36.59
3	RSM	1500	60	130	31.22
	ANFIS	1500	60	130	37.56

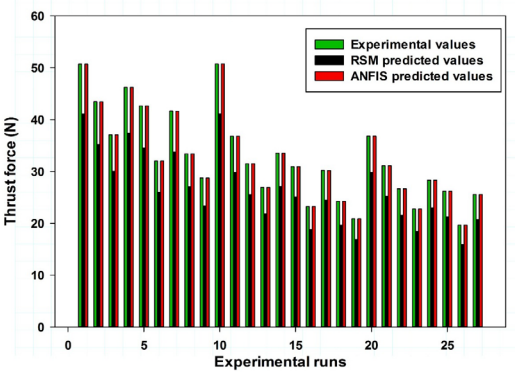

Figure 18: Experimental results of thrust force compared with those of RSM and ANFIS models

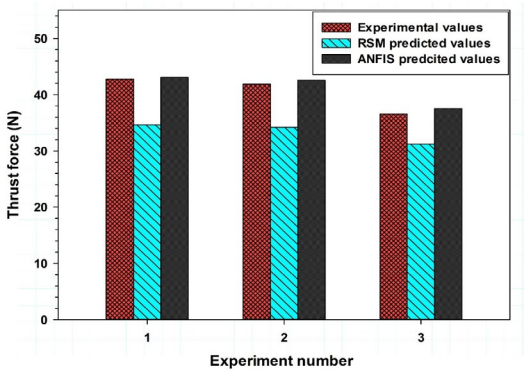

Figure 19: Confirmation test results for thrust force in drilling F-Ep composites

CONCLUSION

In the present work, silane treated F-Ep composites with varying fiber loading were successfully fabricated and tested for their vibration properties. The free vibration test revealed that an increase in fiber content increased the natural frequency and damping property of the composites. Of the prepared F-Ep laminates, 45F-Ep emerged as a superior one.

Drilling on F-Ep composites was performed and the measured thrust force ranged from 19.66 to 50.75 N. From the ANOVA, it was observed that spindle speed is the most significant factor that influenced the output response. The minimum thrust force was generated when the drilling of the F-Ep composite was performed at high spindle speed with high feed rate using a low drill point angle tool. Thus, delamination can be reduced and good surface finish of the drill hole can be anticipated. Fiber pull-out, fibre fracture, matrix debris and fiber projections are the major observations concluded from the FESEM analysis.

The RSM regression model and ANFIS model were developed to predict the thrust force generated while drilling the F-Ep composite. The latter technique was found to be more efficient in predicting the thrust force than the former, as the R^2 value of the ANFIS model is 0.988. Moreover, the confirmation test for the selected input range indicated the same, and the obtained experimental results are in close agreement with those predicted by the ANFIS model, followed by those of RSM.

REFERENCES

[1] S. V. Kumar, K. S. Kumar, H. S. Jailani and G. Rajamurugan, *Mater. Res. Express*., **7**, 085302 2020, https://doi.org/10.1088/2053-1591/abaea5

[2] S. V. Kumar, B. Suresha, G. Rajamurugan and A. Megalingam, *Mater. Res. Express*., **6**, 015307 (2018), https://doi.org/10.1088/2053-1591/aae5dc

[3] V. K. Shettahalli Mantaiah, *J. Nat. Fibers*, **19**, 12415 (2022), https://doi.org/10.1080/15440478.2022.2060404

[4] S. M. Vinu Kumar, C. Sasikumar, E. Sakthivelmurugan and J. P. Rishi, *Mater. Technol*., **55**, 851 (2021), https://doi.org/10.17222/mit.2021.256

[5] S. V. Kumar and H. Singh, *Indian J. Fibre Text*., **48**, 326 (2023), https://doi.org/10.56042/ijftr.v48i3.6057

[6] R. Jeyakumar, S. M. Vinu Kumar, J. P. Rishi and C. Sasikumar, *Mater. Res*., **27**, e20230543 (2024), https://doi.org/10.1590/1980-5373-MR-2023-0543

[7] R. Rajiev, S. V. Kumar, H. Singh and E. Sakthivelmurugan, *Indian J. Fibre Text*., **48**, 396 (2023), https://doi.org/10.56042/ijftr.v48i4.7640

[8] V. K. Shettahalli Mantaiah, S. K. Kallippatti Lakshmanan and S. Kaliappagounder, *J. Nat. Fibers*, **19**, 10367 (2022), https://doi.org/10.1080/15440478.2021.1993504

[9] S. M. Vinu Kumar, N. Manikandaprabu, N. Babu and C. Sasikumar, *Cellulose Chem. Technol*., **58**, 101 (2024), https://doi.org/10.35812/CelluloseChemTechnol.2024.58.10

[10] E. Sakthivelmurugan, G. Senthilkumar, S. M. Vinu Kumar and H. Singh, *Cellulose Chem. Technol*., **57**, 399 (2023), https://doi.org/10.35812/CelluloseChemTechnol.2023.57.35

[11] P. K. Bajpai and I. Singh, *J. Reinf. Plast. Compos*., **32**, 1569 (2013), https://doi.org/10.1177/0731684413492866

[12] H. Rezghi Maleki, M. Hamedi, M. Kubouchi and Y. Arao, *Mater. Manuf*., **34**, 283 (2019), https://doi.org/10.1080/10426914.2018.1532584

[13] A. Lotfi, H. Li and D. V. Dao, *J. Nat. Fibers*, **17**, 1264 (2018), https://doi.org/10.1080/15440478.2018.1558158

[14] N. Rajini, J. W. Jappes, S. Rajakarunakaran and P. Jeyaraj, *J. Compos. Mater*., **47**, 3105 (2013), https://doi.org/10.1177/0021998312462261

[15] A. Etaati, S. A. Mehdizadeh, H. Wang and S. Pather, *J. Reinf. Plast. Compos.*, **33**, 330 (2014), https://doi.org/10.1177/0731684413512228
[16] K. S. Kumar, I. Siva, N. Rajini, P. Jeyaraj and J. W. Jappes, *J. Reinf. Plast. Compos.*, **33**, 1802 (2014), https://doi.org/10.1177/0731684414546782
[17] H. Jena, A. K. Pradhan and M. K. Pandit, *Adv. Compos. Lett.*, **23** (2014), https://doi.org/10.1177/096369351402300103
[18] M. Uthayakumar, V. Manikandan, N. Rajini and P. Jeyaraj, *Mater. Des.*, **64**, 270 (2014), https://doi.org/10.1016/j.matdes.2014.07.020
[19] C. Bennet, N. Rajini, J. W. Jappes, I. Siva, V. Sreenivasan and S. Amico, *J. Reinf. Plast. Compos.*, **34**, 293 (2015), https://doi.org/10.1177/0731684415570683
[20] S. Arulmurugan and N. Venkateshwaran, *Polym. Polym. Compos.*, **24**, 507 (2016), https://doi.org/10.1177/096739111602400709
[21] C. Arvinda Pandian and H. Siddhi Jailani, *Polym. Bull.*, **75**, 1997 (2018), https://doi.org/10.1007/s00289-017-2139-3
[22] K. Senthilkumar, N. Saba, M. Chandrasekar, M. Jawaid, N. Rajini *et al.*, *Constr. Build. Mater.*, **195**, 423 (2019), https://doi.org/10.1016/j.conbuildmat.2018.11.081
[23] K. Sumesh, K. Kanthavel and S. Vivek, *Mater. Res. Express.*, **6**, 045318 (2019), https://doi.org/10.1088/2053-1591/aaff1a
[24] G. R. Kumar, V. Hariharan and S. Saravanakumar, *J. Nat. Fibers*, **18**, 531 (2021), https://doi.org/10.1080/15440478.2019.1636740
[25] M. Chandrasekar, I. Siva, T. S. M. Kumar, K. Senthilkumar, S. Siengchin *et al.*, *J. Polym. Environ.*, **28**, 2789 (2020), https://doi.org/10.1007/s10924-020-01814-8
[26] G. Rajamurugan, S. Aravindraj and P. E. Sudhagar, *J. Nat. Fibers*, **19**, 2885 (2022), https://doi.org/10.1080/15440478.2020.1835782
[27] A. A. Nasir, A. Azmi and A. Khalil, *Measurement*, **75**, 298 (2015), https://doi.org/10.1016/j.measurement.2015.07.046
[28] T. B. Yallew, P. Kumar and I. Singh, *J. Mater.: Des. Appl.*, **230**, 888 (2016), https://doi.org/10.1177/1464420715587750
[29] V. K. Mahakur, S. Bhowmik and P. K. Patowari, *Proc. Ins. Mech. Eng. Part C*, **236**, 6232 (2022), https://doi.org/10.1177/09544062211063752
[30] B. Kavad, A. Pandey, M. Tadavi and H. Jakharia, *Proc. Technol.*, **14**, 457 (2014), https://doi.org/10.1016/j.protcy.2014.08.058
[31] G. C. Onwubolu and S. Kumar, *J. Mater. Process. Technol.*, **171**, 41 (2006), https://doi.org/10.1016/j.jmatprotec.2005.06.064
[32] S. Jayabal, U. Natarajan and U. Sekar, *Int. J. Adv. Manuf. Technol.*, **55**, 263 (2011), https://doi.org/10.1007/s00170-010-3030-7
[33] T. Valarmathi, K. Palanikumar, S. Sekar and B. Latha, *Mater. Manuf.*, **35**, 469 (2020), https://doi.org/10.1080/10426914.2020.1711931
[34] A. Karthik and P. Sampath, *Indian J. Fibre Text. Res.*, **45**, 267 (2020), https://doi.org/10.56042/ijftr.v45i3.27238
[35] C. Anjinappa, O. S. Ahmed, M. Abbas, A. A. Alahmadi, M. Alwetaishi *et al.*, *Processes*, **10**, 2735 (2022), https://doi.org/10.3390/pr10122735
[36] A. Kumar, H. Singh and V. Kumar, *Mater. Manuf.*, **33**, 1483 (2018), https://doi.org/10.1080/10426914.2017.1401727
[37] T. Rajamurugan, C. Rajaganapathy, S. Jani, C. S. Gurram, H. L. Allasi *et al.*, *Adv. Mater. Sci. Eng.*, (2022), https://doi.org/10.1155/2022/9481566
[38] D. S. Tran, V. Songmene and A. D. Ngo, *Neural. Comput. Appl.*, **33**, 11721 (2021), https://doi.org/10.1007/s00521-021-05869-z
[39] D. Karaboga and E. Kaya, *Artif. Intell. Rev.*, **52**, 2263 (2019), https://doi.org/10.1007/s10462-017-9610-2
[40] A. Azmi, *Adv. Eng. Softw.*, **82**, 53 (2015), https://doi.org/10.1016/j.advengsoft.2014.12.010
[41] N. Manikandan, K. Balasubramanian, D. Palanisamy, P. Gopal, D. Arulkirubakaran *et al.*, *Mater. Manuf.*, **34**, 1866 (2019), https://doi.org/10.1080/10426914.2019.1689264
[42] G. Özden, M. Ö. Öteyaka and F. M. Cabrera, *J. Thermoplast. Compos. Mater.*, **36**, 493 (2023), https://doi.org/10.1177/08927057211013070
[43] S. T. Kumaran, T. J. Ko, R. Kurniawan, C. Li and M. Uthayakumar, *J. Mech. Sci. Technol.*, **31**, 3949 (2017), https://doi.org/10.1007/s12206-017-0741-9
[44] M. Marani, V. Songmene, M. Zeinali, J. Kouam and Y. Zedan, *Neural. Comput. Appl.*, **32**, 8115 (2020), https://doi.org/10.1007/s00521-019-04314-6
[45] S. M. Vinu Kumar, C. Sasikumar, E. Sakthivelmurugan and J. Rishi, *Mater. Technol.*, **55**, 851 (2021), https://doi.org/10.17222/mit.2021.256
[46] E. Sakthivelmurugan, G. Senthil Kumar, S. M. Vinu Kumar and H. Singh, *J. Braz. Soc. Mech. Sci. Eng.*, **45** (2023), https://doi.org/10.1007/s40430-023-04339-y
[47] M. Rajesh and J. Pitchaimani, *J. Reinf. Plast. Compos.*, **35**, 228 (2016), https://doi.org/10.1177/0731684415611973
[48] M. Rajesh, S. P. Singh and J. Pitchaimani, *J. Ind. Text.*, **47**, 938 (2018), https://doi.org/10.1177/1528083716679157
[49] E. Sakthivelmurugan and S. M. Vinu Kumar, *Mater. Res.*, **26**, e20230108 (2023), https://doi.org/10.1590/1980-5373-MR-2023-0108